Additive Manufacturing 25 (2019) 477–484

Contents lists available at ScienceDirect

Additive Manufacturing

journal homepage: www.elsevier.com/locate/addma

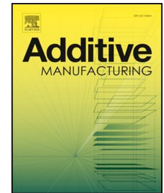

Reactive material jetting of polyimide insulators for complex circuit board design

Fan Zhang, Ehab Saleh, Jayasheelan Vaithilingam, You Li, Christopher J. Tuck, Richard J.M. Hague, Ricky D. Wildman, Yinfeng He*

Faculty of Engineering, University of Nottingham, University Park, NG7 2RD, Nottingham, United Kingdom

ARTICLE INFO

Keywords:
3D print
Additive manufacturing
Printed electronics
Polyimide
Inkjet

ABSTRACT

Polyimides are a group of high performance thermal stable dielectric materials used in diverse applications. In this article, we synthesized and developed a high-performance polyimide precursor ink for a Material Jetting (MJ) process. The proposed ink formulation was shown to form a uniform and dense polyimide film through reactive MJ utilising real-time thermo-imidisation process. The printed polyimide film showed a permittivity of 3.41 and degradation temperature around 500 °C, both of which are comparable to commercially available polyimide films. Benefiting from the capability of being able to selectively deposit material through MJ, we propose the use of such a formulation to produce complex circuit board structures by the co-printing of conductive silver tracks and polyimide dielectric layers. By means of selectively depositing 4 μm thick patches at the cross-over points of two circuit patterns, a traditional double-sided printed circuit board (PCB) can be printed on one side, providing the user with higher design freedom to achieve a more compact high performance PCB structure.

1. Introduction

Material Jetting (MJ) is an advanced, high resolution Additive Manufacturing (AM) method, which can be used to produce structures by stacking up material droplets. Benefiting from the capability to include multiple drop-on-demand inkjet print heads in a single machine, MJ allows co-printing of various functional materials in picolitre droplets by selectively depositing them to the target location to form either 2D or 3D structures [1,2]. In the past decade, there has been growing interest in manufacturing electronics, especially printed circuit boards (PCB) created through the MJ process. The use of MJ for circuit board manufacturing can simplify the whole production process compared with conventional PCB manufacturing methods, reducing the material waste and production cost especially for low volume products [3] and also providing great design freedom [3–7]. This will allow the user to produce bespoke products such as flexible or disposable elecronics [8].

With the recent advances in MJ of electronic circuits, various types of electronics have been printed including, transistors [9], capacitors [10], inductors [11], flexible circuit board [12], etc. All of these studies are based on single-sided circuit board designs. Single-sided circuit boards have limited circuit design freedoms and circuit densities; in order to avoid a short circuit failure, the conductive tracks are not allowed to have any intersections in their route. In industrial manufacturing, double sided PCB circuit is commonly used, the conductive tracks are usually placed on both sides of the board to achieve increased circuit density and a more compact structure. In 2014, Andersson et al. fabricated workable double-sided PCBs by laminating two separately printed single-sided PCBs together, presenting one solution to this problem [13].

In this paper, a simpler solution to preparing double-sided PCBs is proposed. Instead of separating the whole circuit using a dielectric plate, as for a double-sided PCB, here in order to achieve a high circuit density, an insulating material is selectively deposited at the cross-over points, creating an insulating bridge for the circuit. When printing these local insulators, it is important to control film topography and to eliminate defects such as “coffee stain” drying [4], cracking [4] and delamination [8]. Therefore, a reliable insulating material with superior dielectric properties and film qualities is required. Consequently, Polyimides (PIs) were selected as the insulating material. PIs are important engineering polymers that are well known for their excellent thermal stability, chemical resistance, mechanical and electrical properties [14,15,12]. It is a particularly attractive material in the microelectronic industry, and has important applications in interlayer dielectrics [16] and as protective layers in integrated circuit fabrication

* Corresponding Author.
E-mail address: ezzyh2@nottingham.ac.uk (Y. He).

https://doi.org/10.1016/j.addma.2018.11.017
Received 20 August 2018; Received in revised form 13 November 2018; Accepted 17 November 2018
Available online 22 November 2018
2214-8604/ © 2018 The Authors. Published by Elsevier B.V. This is an open access article under the CC BY license (http://creativecommons.org/licenses/BY/4.0/).

and microelectromechanical system (MEMS) devices [17]. The traditional method to prepare PIs samples is through a two-step process, in which PI precursor poly(amic) acid (PAA) solution is casted and cured upon heating or chemical treatment [18], followed by being manufactured into samples using lithography [20]. In our previous work, we reported a one-step inkjet printing process to prepare ultra-thin PI insulating layers during which PAA solutions were jetted and thermo-imidised simultaneously, and applied to the fabrication of parallel plate capacitors [21]. However, some drawbacks, such as uncontrollable film thickness and coffee-ring effects, were observed for the previous polyimide ink, which may lead to electrical failure. In this article, a new method for preparing inkjet printable polyimide is demonstrated. This method will avoid the drawbacks of previous attempts and form dense films with controllable dimensions and improved topography, which served as great local insulator in the fabrication of circuit equivalent to double-sided PCBs.

2. Methodology

2.1. Ink preparation

All chemicals were purchased from Sigma-Aldrich (UK) and used as received. To prepare the PI ink, 7.7 mmol (3.17 g) of 4,4′-(4,4′-isopropylidenediphenyl-1,1′-diyldioxy) dianiline (BAPP), 10.2 mmol (1.00 g) of maleic anhydride (MA), 10 g of 1,2-dimethoxyethane (EDM) and 10 g of 1-methyl-2-pyrrolidinone (NMP) were mixed and stirred in a 50 mL round bottom flask at 400 rpm for 4 h at room temperature (Fig. 1). After that, 2.55 mmol (0.82 g) of benzophenone-3,3′,4,4′-tetracarboxylic dianhydride (BPDA) was added into the mixture and stirred for another 4 h at room temperature. The resultant ink was a dark yellow solution containing 20 wt% of polyamic acid (PAA). Silver nanoparticle (∼ 38 wt%) ink was purchased from Advanced Nano Products Co. Ltd and used for the printing of the conductive tracks.

2.2. Printability assessment

To assess the printability of the PAA precursor solution, a printing indicator Z was introduced [22], which is defined by Eq. 1

$$Z = \frac{\sqrt{\rho r \gamma}}{\mu} \tag{1}$$

where ρ is the density ($g{\cdot}cm^{-3}$), r is the orifice diameter (μm), γ is the surface tension of the fluid ($mN{\cdot}m^{-1}$) and μ is the viscosity of the ink (mPa·s). When Z falls between 1 and 10, an ink is considered to be printable [23]. To determine the Z number, the viscosity of the ink was assessed using a parallel plate rheometer (Malvern Kinexus Pro) with a shear rate sweep between 10 and 1000 s^{-1} at 50 °C, while the surface tension was measured at 50 °C using a Kruss DSA100S pendant drop shape analyser.

The printing indicator Z of the ink at 50 °C was calculated to be 3.98, as shown in Table 1. This ink was subsequently demonstrated to be printable.

2.3. Material jetting

A Dimatix DMP 2800 printer (Fujifilm) was used to carry out the printing of PI ink. The prepared ink containing 20 wt% PAA was filtrated (using HPLC Nylon 5.0 μm syringe filters, Cole-Parmer) and 3 mL of ink was injected into the cartridge (DMC-11610, 10 pL). The Dimatix printhead consisting 16 nozzles (21 μm nozzle diameter) was used for jetting. Stable droplets were obtained at a cartridge temperature of 50 °C and printing voltage of 26 V. To study the printing quality, individual droplets and squares were printed on glass substrates (microscope slides, Cole-Parmer), which were heated and held at different temperatures (120 °C, 150 °C and 180 °C) using a thin film heater (KHLV-103/5 Kapton insulated flexible heater, Omega) during printing to enable the solvent evaporation and thermal imidisation.

To demonstrate the capability of producing a single sided circuit board with two overlapped circuit patterns through material jetting, a demonstrator was produced by subsequently printing circuit one followed by polyimide insulator deposited on the designed overlap locations and then circuit pattern two (as shown in Fig. 2). The printhead height was set to 1000 μm above the glass substrate and elevated for 10 μm after printing one layer of silver ink or PAA ink.

2.4. Surface morphology

A Nikon Eclipse LV100ND optical microscope was used to characterise the droplet sizes and the general surface morphology of printed samples. Surface topography was characterised using a Bruker GT-I 3D Optical Microscope. The cross-sections of the printed and cast films were observed using a Hitachi TM3030 tabletop Scanning Electron Microscope (SEM).

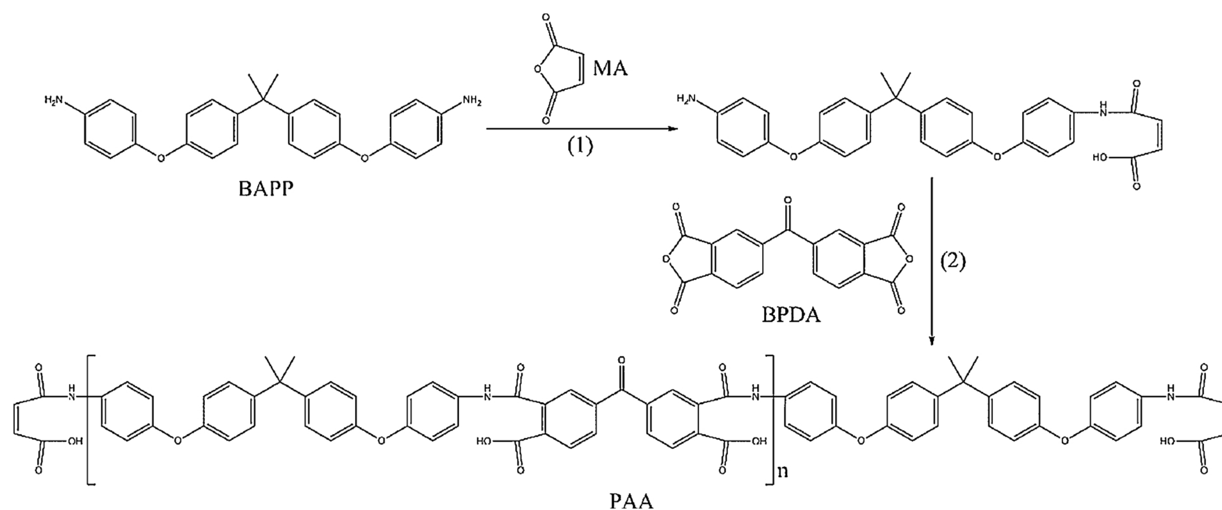

Fig. 1. Chemical reaction route to prepare polymerise PAA as the precursor for inkjet printable PI ink. (1)10.2 mmol of BAPP containing 20.4 mmol of amine groups, then 10.2 mmol of MA was added which reacted with 10.2 mmol of the amine groups in BAPP; (2) BPDA was then added in to react with remaining amine groups in BAPP and form PAA precursor.

Table 1
Printability index Z of the PI ink.

Sample	Nozzle Diameter (μm)	Density (g/cm^3)	Viscosity (at 1000s^{-1}) (mPa S)	Surface Tension (mN/m)	Z (Oh^{-1})
PI ink	21	1.03	6.73	33.13	3.98

2.5. Characterisations of printed PI

The degree of imidisation D was characterised using Fourier Transform-Infrared Red (FT-IR) spectroscopy, during which a PerkinElmer Frontier FT-IR Spectrometer with an attenuated total reflectance (ATR) accessory was employed to scan the range from 1000 cm^{-1} to 2000 cm^{-1} at a step length of 4 cm^{-1}. The thermal stability of the printed PI was characterised using a PerkinElmer Thermogravimetry Analysis (TGA) 4000 machine, during which the sample was heated from 30 °C to 750 °C at a heating rate of 40 °C per minute in a nitrogen environment. An LCR meter (Hameg®, HM8018) at 1 kHz was used to measure and calculate the dielectric constant of the printed PI films.

3. Results and discussions

3.1. Effects of substrate temperature on surface morphology

Once the proposed inkjet printable PAA precursor ink was ejected and deposited onto the target location, the conversion from PAA precursor ink into PI was initialised. Such a process involves a physical transformation in that the solvent in the ink evaporates and the polymer content starts to precipitate to form a solid structure. Meanwhile, the PAA precursor transforms into PI through a thermal imidisation reaction during which water molecules condensates from PAA and form new covalent bonding [16,21]. Both transformations take place simultaneously and the solvent acts as an effective plasticizer for the imidisation reaction [16].

When printing a solvent based ink, the substrate temperature has been found to be one of the key factors that determines the surface morphology of the printed structure [21]. To study the effects of substrate temperature on the deposited ink droplets, three substrate temperatures (120 °C, 150 °C and 180 °C) were chosen. The cross-section profile of the printed and solidified PI was measured and shown in Fig. 3.

It can be observed from Fig. 3 that under the higher substrate temperature regime, the overall diameter of the printed and solidified droplets decreased, but the thickness increased. This is because after the impact of a droplet onto the substrate, the ink tends to relax and spread outwards to reach an equilibrium contact angle. However, higher substrate temperatures accelerate the solvent evaporation and therefore the deposited ink droplet had less time to spread to reach equilibrium before fully solidified, resulting in a reduced diameter of the deposited and solidified droplet [21,24]. Less spreading also leads to a higher density of material per unit area, resulting in a thicker layer post-solidification. Compared to our previous PI ink formulation [21], these droplets also showed no obvious coffee ring effects [26–28]. This is likely due to the high PAA concentration and the EDM/NMP dual-solvent system, which will tend to create a Marangoni flow on the droplet surface, and suppress the outward capillary flow that pushes the material to the droplet edge [29].

The effects of substrate temperature on the surface morphology of the printed PI films (5 mm x 5 mm) are illustrated in Fig. 4(a), and their corresponding surface roughness R_z values are measured and shown in Table 2. To keep the consistency of the results, all films were printed with a droplet spacing of 20 μm, which was determined as likely to be suitable for this ink from our previous studies [21]. It can be concluded from the results that a higher substrate temperature improves the surface quality of the printed film as lower roughness R_z and “sharper” film edges were observed. Such an effect was owing to the competition between ink evaporation and merging [4]. When the ink was printed at lower temperature, the printed ink stays in a liquid form for longer period of time, which may partially re-dissolve the previously deposited layer, forming bulge-like defections on film due to surface tension and increased unevenness of the printed surface [30].

Multi-layer printing demonstrated the capability of creating 3D structures through printing and polymerization of our proposed PAA precursor formulation. As shown in Fig. 4(a) and Table 2, average surface roughness R_z increased with increasing number of layers, suggesting that multi-layer printing would amplify heterogeneities as the film was built up. But under a substrate temperature of 180 °C, the increment of surface roughness was better controlled compared with lower substrate temperatures.

Fig. 4(b) and (c) show the cross sectioned SEM images of PI films

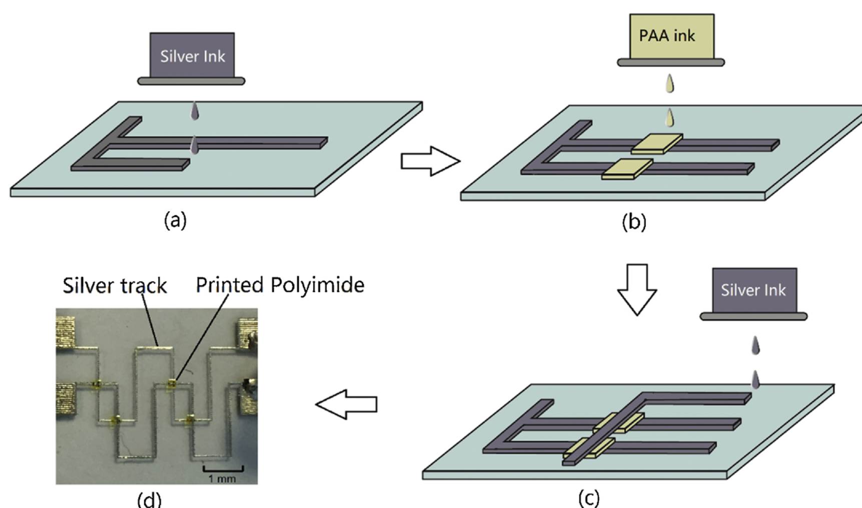

Fig. 2. A schematic of producing complex circuit board structures by using reactive material jetting technique to co-printing of silver conductive track and polyimide insulator.

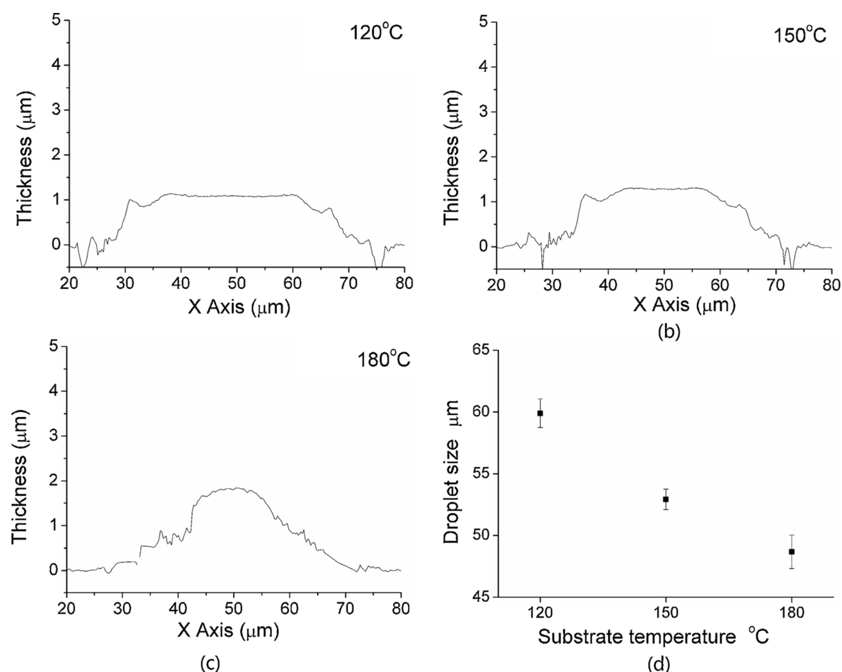

Fig. 3. Cross-sectional surface profiling results of droplets deposited on glass by material jetting under substrates temperature of (a) 120 °C, (b) 150 °C, and (c) 180 °C; (d) and their corresponding deposited drop diameters.

prepared by MJ and traditional casting method. The film in Fig. 4 (b) was the PI structure produced by sequentially depositing and curing 30 layers of the ink by MJ, while that in Fig. 4 (c) was prepared by the drop casting method (directly casting the same ink onto a 180 °C glass surface). Both methods achieved dense PI films with no signs of pinhole defects through the cross-section, suggesting MJ is a reliable manufacturing method to produce PI based structures with a quality comparable to that used in industry.

3.2. Thermal imidisation of the PI ink

The ink containing PAA was directly deposited onto preheated glass substrates, during which solvent evaporation and thermal imidisation happened simultaneously. The degree of imidisation of the printed PI was tracked using FTIR. According to our previous results, the solvent evaporation steps finished within 1500 ms, while the thermal imidisation process (Fig. 5(a)) required much longer time to reach a reasonable conversion [21].

Fig. 5(b) shows the IR spectra of PAA precursor and the thermal imidised PI film. A sharp peak at around 1375 cm^{-1} (peak ‘a’) indicated the conversion of PAA into PI, which was assigned to the C–N stretch of the imide group observed in PI but not existing in PAA precursor. The peak at 1230 cm^{-1} (peak ‘b’) assignable as the C–O stretch of phenyl ether was selected as the reference peak, as this phenyl-O-phenyl structure remains the same as before and after the imidisation reaction [16]. By comparing the peak height of the two peaks after normalization of the peak intensity using the reference peak at 1230 cm^{-1}, the degree of imidisation D can be ascertained using the following equation [16,31,32].

$$D = \frac{a/b\,[sample] - a/b\,[init]}{a/b\,[imid] - a/b\,[init]} \times 100\% \quad (2)$$

where *[sample]* stands for the PAA films heat treated at different conditions; *[init]* is the PI ink before imidisation; *[imid]* is the reference PI film which is fully cured at 300 °C for 30 min.

Fig. 5(c) shows the conversion of PAA precursor into PI under different substrate temperatures and post treatment. As the substrate temperature increased from 120 °C to 180°C, D for the printed PI films increased from 34.3% to 89.8%. These low conversion values at 120 °C can be attributed to the insufficient energy for the imidisation reaction. To improve the conversion of PAA into PI, the printed films were left on the substrate for additional 15 min, which significantly increased the imidisation conversion. For a substrate temperature of 120 °C, this conversion led to a doubling of imidisation to 67.6%. For 180 °C, the printed PAA was almost fully imidised, suggesting that an additional 15 min of heating or other post-heating treatment will be beneficial for the PAA to convert into PI.

The thermal imidisation process can also be confirmed using TGA. As illustrated in Fig. 5(d), the printed PAA precursor showed an 11.4% weight loss at 150 °C–350 °C, larger than the theoretical value of 5.34 wt%, indicating the loss of water and evaporation of remaining solvents during the imidisation process. For a printed PI film printed and post-treated by heating at 180 °C for 15 min, no obvious weight loss was found at below 400 °C, implying a good thermal stability of inkjet printed polyimide parts.

4. Printed Pi Films as dielectric insulators

4.1. Dielectric constant of the printed PI film

A PI film (10 mm × 10 mm) with a thickness of 150 μm was printed and sandwiched between two polished Aluminum plates and the capacitance of it was measured using an LCR meter (Hameg®, HM8018) at 1 kHz. The film was dried in a convection oven at 60 °C for 24 h before the test, and the capacitance value was measured to be 20.14 ± 0.50 pF at ambient environment. Since the capacitance was measured, the relative permittivity can then be calculated through a generally used parallel plate capacitance equation as shown in Eq. 3. The relative permittivity of the printed polyimide was 3.41 ± 0.09, which is comparable to a commercial Kapton® polyimide film with a capacitance of 3.5.

$$C = \frac{\varepsilon_r \varepsilon_0 A}{d} \rightarrow \varepsilon_r = \frac{Cd}{\varepsilon_0 A} \quad (3)$$

$$\varepsilon_r = \frac{Cd}{\varepsilon_0 A} = \frac{150 \times 10^{-6} \times (20.14 \pm 0.50) \times 10^{-12}}{8.85 \times 10^{-12} \times 0.0001} = 3.41 \pm 0.09$$

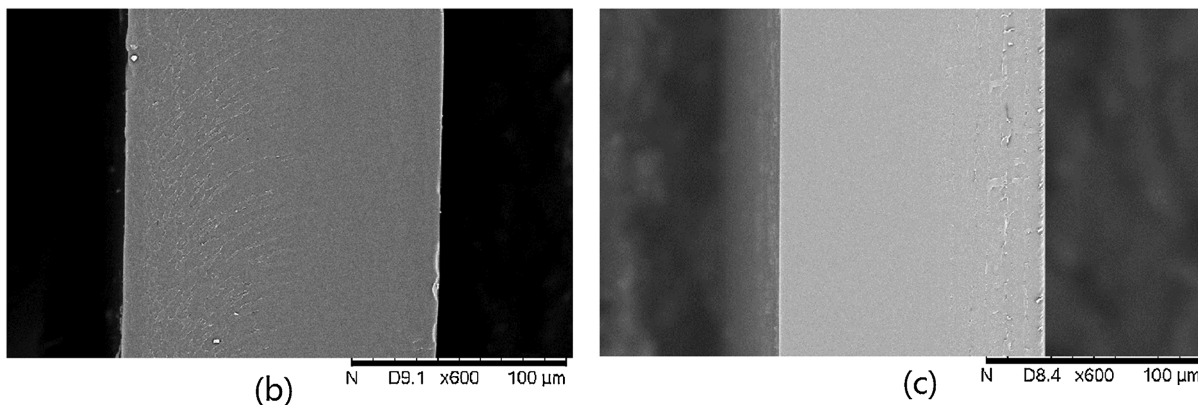

Fig. 4. (a) Surface morphology results of printed PI films (5 mm x 5 mm) under different substrate temperatures (120 °C, 150 °C and 180 °C) and number of layers (1, 3 and 6 layers); SEM micrographs of the cross sections of two PI films prepared by (b) inkjet printing and (c) casting.

Table 2
Surface roughness R_z of the printed PI films (5 mm x 5 mm) under different substrate temperatures (120 °C, 150 °C and 180 °C) and number of layers (1, 3 and 6 layers).

R_z	120 °C	150 °C	180 °C
1 layer	4.81 ± 1.02 µm	2.97 ± 0.57 µm	1.29 ± 0.27 µm
3 layers	4.36 ± 2.09 µm	3.87 ± 0.69 µm	3.09 ± 1.12 µm
6 layers	7.91 ± 2.39 µm	5.83 ± 2.86 µm	3.72 ± 1.04 µm

where C is the capacitance, d is the thickness, A is the area, and ε_0 is the dielectric constant of free space.

4.2. Selective deposition of PI insulators onto silver tracks

A series of square PI films with four different dimensions (200 × 200 µm, 300 × 300 µm, 400 × 400 µm and 500 × 500 µm) sandwiched by two crossing silver conductive tracks were printed using MJ by subsequently printing Silver- > PI- > Silver layer (Fig. 6(a)). The results showed that PI squares with all sizes successfully worked as

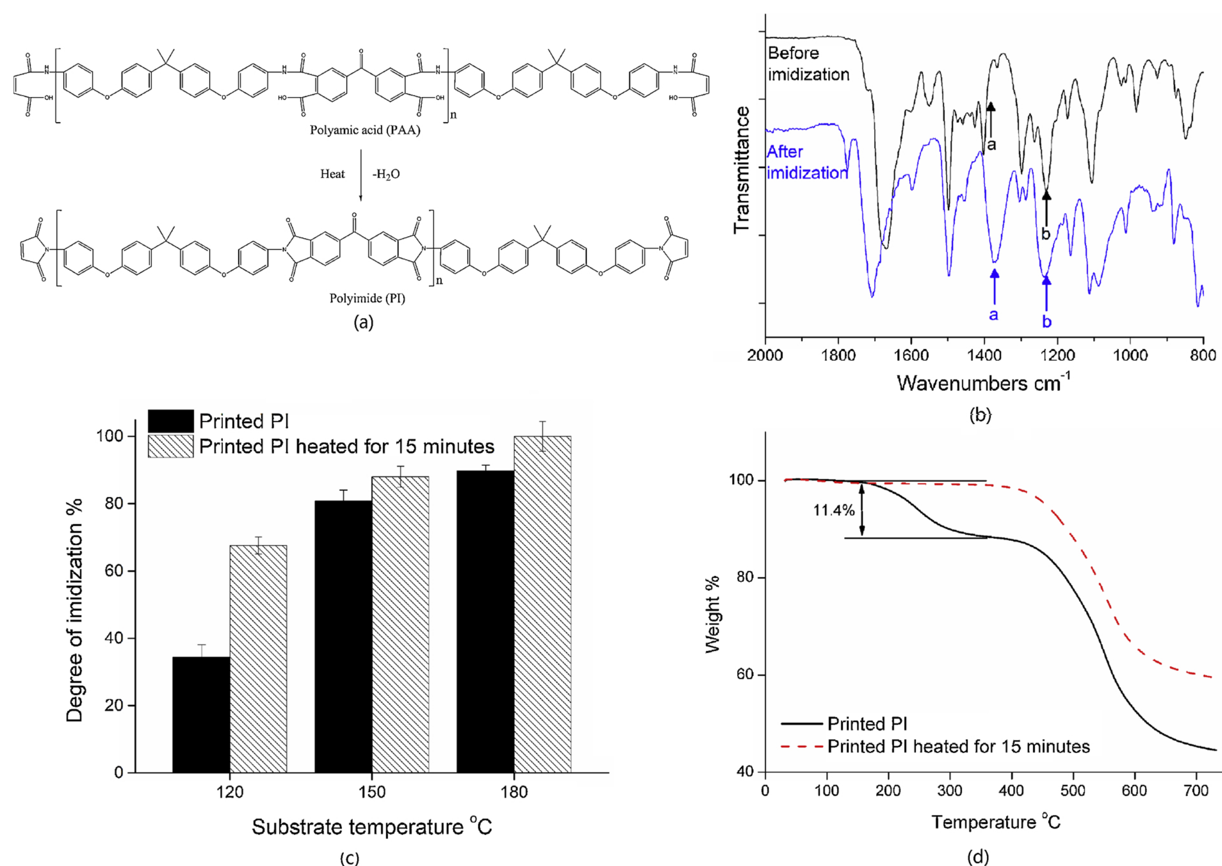

Fig. 5. (a) Thermal imidisation process of forming PI from its precursor PAA; (b) FT-IR spectra of PAA precursor ink and PI after the thermal imidisation process, two peaks were identified at 'a' around 1375 cm^{-1} (C–N stretch of the imide group) and at 'b' 1230 cm^{-1} (C–O stretch of phenyl ether), and used to determine the degree of conversion to PI; (c) PAA precursor was printed onto glass substrate and converted into PI under three different temperatures (120 °C, 150 °C and 180 °C). The sample for assessing imidisation degree was characterized by FTIR directly after solidification and also with 15 min post-process with heat treatment. (d) Effect of an additional 15 min heating at 180 °C on the thermal stability of the printed PI films.

dielectric insulators.

The silver ink track printed on top of the square PI insulator showed less continuity on those with smaller dimensions than those with larger, since the silver ink tended to stack at the edge of the PI beneath the silver track. When printing a small pattern, all the droplets required to form the pattern will be deposited onto the target locations within very short period of time, leaving them limited time to dry and pin themselves. These droplets will then have time to merge together before drying to form a larger droplet. Owing to surface tension, they tend to form hemispherical cap than a flat film surface, which will cause the solidified polymer end up with a bump cross-section. This conclusion can be confirmed by the surface profiling results of printed PI squares as shown in Fig. 6(c), from which it can be observed that a square of 200 × 200 μm in size shows significant difference in thickness across the vertical direction, resulting in a steep top edge. As a result, the silver ink deposited at the top edge would flow down the slope before solidifying, causing this stacking problem. An increased square size significantly reduced this problem, probably due to the relatively shorter contact-line.

A series of demonstrators were shown in Fig. 6(d–f) to demonstrate the capability of reactive material jetting of PI for electronic printing applications. Fig. 6(d) comprised of two crossed conductive tracks with 500 × 500 μm PI insulators in between, which successfully turned on the LED light without short circuit. Instead of separating the whole area between two conductive layers such as the case in double layer PCB, the inkjet printing of customized PI insulators would be a much easier and cheaper way to do the same work but in a single layer.

5. Discussion

The use of inkjet 3D printing process for electronics production has been a popular research area in recent years as it provides the user a technique to quickly produce small batch of bespoke electronic such as circuit board with much lower overhead cost than traditional manufacturing method. Most of the current researches on printed circuit still showed limited capability to produce fully inkjet printed complex circuit board with high performance dielectric material [9–11,15,32–34]. Andersson et al. [13] produced printed complex double sided PCB with paper and a copper rivet integrated after printing to connect the circuits from both sides. Macdonald et al. [35] demonstrated the use of 3D printing for making complex 3D circuit structure by sequentially using multiple AM techniques to achieve the final structure. In this paper, we aim to present an efficient and continuous process to 3D print complex circuits with conductive tracks together with high performance polyimide dielectric layer. The conductivity of the inkjet printed silver track is around 13.6 to 22.5 μΩ cm as reported in our previous research [36]. This novel approach suggested that reactive material jetting of polyimide insulators can be a potential technique to be used in general material jetting process to design and fabrication of customized high performance complex circuits. Polyimide, as an engineering polymer that has high thermal stability (up to 400 °C) and chemical resistance, faced a lot of challenges when applying to AM processing. The PAA ink prepared in this paper is a precursor which is much more processing friendly than its final form: polyimide. The final imidisation conversion step was introduced after layer deposition to form the polyimide product. Although this formulation was designed for material jetting

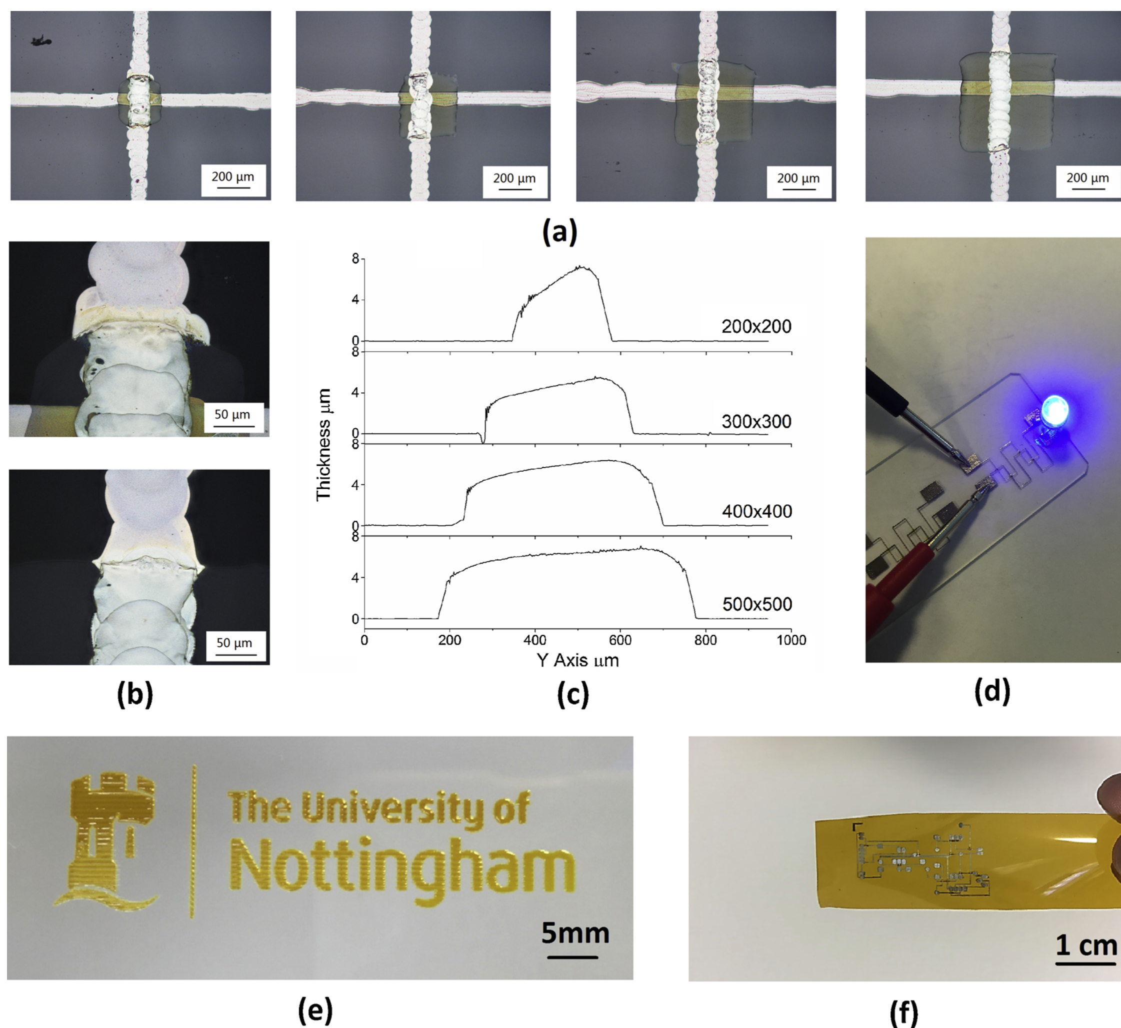

Fig. 6. (a) Perpendicularly crossed conductive tracks separated by printed PI films with dimensions of 200 × 200 µm, 300 × 300 µm, 400 × 400 µm and 500 × 500 µm; (b) magnified edge for 200 µm square (top) and 500 µm square (bottom); (c) The profiling of the four printed PI squares with different dimensions (200 × 200 µm, 300 × 300 µm, 400 × 400 µm, 500 × 500 µm) (d) Demonstration of a complex circuit board structure: single-side printed circuits comprising of cross-over conductive tracks with PI dielectric insulators selectively deposited at the cross-over point only (e) A University of Nottingham logo printed to demonstrate the printability for the reactive material jetting of polyimide; (f) a demonstration of silver circuit printed onto reactive material jetted polyimide.

process, the principle of using polymer precursor followed by chemical reaction to process polymer that has high performance but limited processability could be applied in other kinds of AM techniques to help expand the availability of functional polymeric materials for AM.

6. Conclusions

In this paper, specifically positioned PI insulators were successfully prepared using an inkjet printing method from its precursor PAA. FTIR results showed that printed PAA droplets could convert to PI by heating at 180 °C for over 15 min, potentially allowing for the printing to be part of a continuous process. The printability of PAA ink was studied, with the effects of substrate temperatures on the droplet formation and surface morphology of the samples examined. Compared to the PAA ink used in our previous work [21], this updated version of PAA ink showed no obvious coffee ring effects. It was observed that an increased substrate temperature reduced the diameter but increased the height of the deposited droplets, meanwhile reduced the surface roughness of the printed films, resulting in "sharper" edges. After determination of the dielectric constant of these printed PI films to be 3.41 ± 0.09, a series of PI insulators (from 200 × 200 µm to 500 × 500 µm in size) were printed to serve as the dielectric layers between two crossed conductive tracks. The results revealed that a printed PI square with extremely small dimensions (200 × 200 µm) could result in an uneven surface and hence a steep edge. A series of demonstrators comprising of two crossed silver conductive tracks with 500 × 500 µm PI insulators in between were printed and proved to work, indicating that this continuous PI printing process could potentially provide a more versatile and efficient way to fabricate complicated single layer circuit instead of using a double layer PCB.

Competing interests

The authors declare no competing interests.

Acknowledgement

This work was supported by the Engineering and Physical Sciences Research Council [grant number EP/I033335/2, EP/N024818/1, EP/P031684/1], funded at the University of Nottingham.

References

[1] ASTM, Standard Terminology for Additive Manufacturing Technology, (2012).
[2] Y. Yang, V. Naarani, Improvement of the lightfastness of reactive inkjet printed cotton, Dyes Pigm. 74 (2006) 154–160.

[3] Y.Y. Sun, et al., Solvent inkjet printing process for the fabrication of polymer solar cells, RSC Adv. 3 (2013) 11925–11934.
[4] Y. He, R.D. Wildman, C.J. Tuck, S.D.R. Christie, S. Edmondson, An investigation of the behavior of solvent based polycaprolactone ink for material jetting, Sci. Rep. 6 (2016) 1–10.
[5] D.H.A.T. Gunasekera, et al., Three dimensional ink-jet printing of biomaterials using ionic liquids and co-solvents, Faraday Discuss. (2016), https://doi.org/10.1039/C5FD00219B.
[6] C. Zhou, Y. Chen, Additive manufacturing based on optimized mask video projection for improved accuracy and resolution, J. Manuf. Process. 14 (2012) 107–118.
[7] L.R. Hart, et al., 3D printing of biocompatible supramolecular polymers and their composites, ACS Appl. Mater. Interfaces 8 (2016) 3115–3122.
[8] V. Sanchez-romaguera, M. Madec, S.G. Yeates, Inkjet printing of 3D metal – insulator – metal crossovers, React. Funct. Polym. 68 (2008) 1052–1058.
[9] Y. Liu, K. Varahramyan, T. Cui, Low-voltage all-polymer field-effect transistor fabricated using an inkjet printing technique, Macromol. Rapid Commun. 26 (2005) 1955–1959.
[10] Y. Liu, T. Cui, K. Varahramyan, All-polymer capacitor fabricated with inkjet printing technique, Solid State Electron. 47 (2003) 1543–1548.
[11] D. Redinger, et al., An ink-jet-deposited passive component process for RFID, IEEE Trans. Electron Devices 51 (2004) 1978–1983.
[12] S. Diaham, M. Locatelli, R. Khazaka, BPDA-PDA polyimide: synthesis, characterizations, aging and semiconductor device passivation, in: M.J.M. Abadie (Ed.), High Performance Polymers - Polyimides Based - From Chemistry to Applications, 2012, https://doi.org/10.5772/2834.
[13] H.A. Andersson, et al., Assembling surface mounted components on ink-jet printed double sided paper circuit board, Nanotechnology 25 (2014).
[14] J.H. Lai, R.B. Douglas, K. Donohoe, Characterization and processing of polyimide thin films for microelectronics application, Ind. Eng. Chem. Prod. Res. Dev. 25 (1986) 38–40.
[15] T. Ogura, T. Higashihara, M. Ueda, Direct patterning of poly(amic acid) and low-temperature imidization using a crosslinker, a photoacid generator, and a thermobase generator, J. Polym. Sci. Part A: Polym. Chem. 47 (2009) 3362–3369.
[16] K. Fukukawa, Y. Shibasaki, M. Ueda, Efficient catalyst for low temperature solid-phase imidization of poly(amic acid), Chem. Lett. 33 (2004) 1156–1157.
[17] Y. Zhang, et al., Thermal imidization of fluorinated poly(amic acid) precursors on a glycidyl methacrylate graft-polymerized Si(100) surface, J. Vac. Sci. Technol. A Vac. Surf. Film 19 (2001) 547.
[18] J.H. Lai, R.B. Douglas, K. Donohoe, Characterization and processing of polyimide thin films for microelectronics application, Ind. Eng. Chem. Prod. Res. Dev. 25 (1986) 38–40.
[20] W.C. Wilson, G.M. Atkinson, Review of Polyimides Used in the Manufacturing of Micro Systems, Nasa, 2007, pp. 1–16.
[21] F. Zhang, et al., Inkjet printing of polyimide insulators for the 3D printing of dielectric materials for microelectronic applications, J. Appl. Polym. Sci. 133 (2016) 1–11.
[22] C. Ainsley, N. Reis, B. Derby, Freeform fabrication by controlled droplet deposition of powder filled melts, J. Mater. Sci. 37 (2002) 3155–3161.
[23] D. Jang, D. Kim, J. Moon, Influence of fluid physical properties on ink-jet printability, Langmuir 25 (2009) 2629–2635.
[24] H. Dong, W.W. Carr, J.F. Morris, Visualization of drop-on-demand inkjet: drop formation and deposition, Rev. Sci. Instrum. 77 (2006).
[26] R.D. Deegan, et al., Capillary flow as the cause of ring stains from dried liquid drops, Nature 389 (1997) 827–829.
[27] R.D. Deegan, et al., Contact line deposits in an evaporating drop, Phys. Rev. E - Stat. Phys. Plasmas Fluids Relat. Interdiscip. Top. 62 (2000) 756–765.
[28] D. Soltman, V. Subramanian, Inkjet-printed line morphologies and temperature control of the coffee ring effect, Langmuir 24 (2008) 2224–2231.
[29] M. Majumder, et al., Overcoming the “Coffee-Stain” Effect by Compositional Marangoni-, (2012).
[30] A.B. Thompson, C.R. Tipton, A. Juel, A.L. Hazel, M. Dowling, Sequential deposition of overlapping droplets to form a liquid line, J. Fluid Mech. 761 (2014) 261–281.
[31] S. Diaham, M.L. Locatelli, T. Lebey, D. Malec, Thermal imidization optimization of polyimide thin films using Fourier transform infrared spectroscopy and electrical measurements, Thin Solid Films 519 (2011) 1851–1856.
[32] T. Ahn, Y. Choi, H.M. Jung, M. Yi, Fully aromatic polyimide gate insulators with low temperature processability for pentacene organic thin-film transistors, Org. Electron. Phys. Mater. Appl. 10 (2009) 12–17.
[33] H.E. Nilsson, H.A. Andersson, A. Manuilskiy, et al., Printed write once and read many sensor memories in smart packaging applications, IEEE Sens. J. 11 (9) (2011) 1759–1767.
[34] T. Carey, S. Cacovich, G. Divitini, et al., Fully inkjet-printed two-dimensional material field-effect heterojunctions for wearable and textile electronics, Nat. Commun. 8 (1) (2017) 1202.
[35] E. Macdonald, R. Salas, D. Espalin, et al., 3D printing for the rapid prototyping of structural electronics, IEEE Access 2 (2014) 234–242.
[36] J. Vaithilingam, et al., Combined inkjet printing and infrared sintering of silver nanoparticles using a swathe-by-swathe and layer-by-Layer approach for 3-dimensional structures, ACS Appl. Mater. Interfaces 9 (2017) 6560.